JACS
JOURNAL OF THE AMERICAN CHEMICAL SOCIETY
Article
pubs.acs.org/JACS

# A General Strategy for Synthesizing Colloidal Semiconductor Zinc Chalcogenide Quantum Rods

Guohua Jia and Uri Banin*

Institute of Chemistry and Center for Nanoscience and Nanotechnology, The Hebrew University of Jerusalem, Jerusalem 91904, Israel

Supporting Information

**ABSTRACT:** Quasi-one-dimensional (1D) semiconductor nanocrystals manifest linearly polarized emission, reduced lasing threshold, and improved charge transport compared with their counterparts such as spherical quantum dots. Present investigations of colloidal semiconductor quantum rods are mainly based on cadmium chalcogenide systems because of their facile synthetic accessibility. However, it is still a big challenge to fabricate quasi-1D zinc chalcogenide nanocrystals with controlled aspect ratios. Here we report a general strategy for synthesizing zinc chalcogenide quantum rods via a colloidal chemical synthetic approach. Unlike the most common growth mechanisms of quasi-1D colloidal nanocrystals such as monomer attachment and particle coalescence, the synthesis of zinc chalcogenide quantum rods is performed by a ripening process starting from their respective ultrathin nanowires through thermodynamically driven material diffusion. We anticipate that this strategy is general and could be applied to other systems to construct quasi-1D nanostructures. Moreover, the presence of cadmium-free (or "green") zinc chalcogenide quantum rods synthesized through this strategy provides a desirable platform for eco-friendly photocatalysis, optoelectronic devices, biolabeling, and other applications.

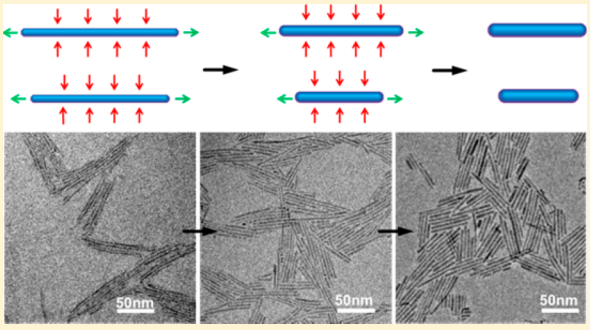


## INTRODUCTION

Selective monomer attachment and coalescence of nanoscale building blocks are important growth mechanisms of quasi-one-dimensional (1D) colloidal nanocrystals.[1−6] On one hand, the growth rates of different facets of a nanocrystal are determined either by the growth behavior of these facets or the binding energy between the facet and the organic surfactant molecule.[7−9] Monomers attach much faster to the high-energy facets than the others, leading to the formation of elongated nanostructures. On the other hand, quantum wires can be produced by coalignment and coalescence from isolated individual nanoscale building blocks via an oriented attachment process.[10−16] However, compared with cadmium chalcogenide (CdS, CdSe, and CdTe) quantum rods, which have been intensively studied,[7−9,17−31] the path to obtaining high-quality zinc chalcogenide quantum rods poses a synthetic challenge, as conventional synthetic routes such as monomer attachment and particle coalescence result in nanocrystals with either low quality or poorly controlled aspect ratios. This is partially due to the stability of different crystal structures of zinc chalcogenide nanocrystals that are not necessarily compatible with the anisotropic growth needed to form quantum rods.

The growth approach of monomer attachment in the presence of phosphonic acids as surfactants in phosphine solvents leads to controlled growth of CdS, CdSe, and CdTe quantum rods with good size distributions and controlled aspect ratios.[17−31] Recently, Manna and co-workers[32,33] developed a versatile sequential cation exchange approach, namely, $Cd^{2+} \rightarrow Cu^{+} \rightarrow Zn^{2+}$, to prepare ZnSe nanorods from CdSe nanorods. However, attempts to use the above-mentioned direct monomer attachment approach to synthesize quasi-1D zinc chalcogenide nanocrystals have been generally unsuccessful, resulting in either polycrystalline or polypod-shaped zinc chalcogenide nanoparticles with poor size distributions.[34−37] It has been demonstrated that alkylamines, rather than phosphines, which act as both surfactant ligands and solvents, are more suitable for synthesizing zinc chalcogenide quantum rods because of the better compatibility between alkylamine ligands and zinc ions.[38−43] However, width control of the zinc chalcogenide quantum rods has not been achieved. In these cases, the thermal decomposition of organometallic precursors produces small ZnSe or ZnS spherical quantum dots. Instead of adopting selective monomer attachment, the produced individual quantum dots coalign and coalesce into elongated nanowires by the oriented attachment mechanism. The widths of the produced nanowires are mainly below 3 nm,[38−40,44−50] suggesting that the limitation of width control of quasi-1D zinc chalcogenide nanocrystals imposed by alkylamines is hard to circumvent.

Unlike the growth mechanisms associated with quantum rods such as monomer attachment and particle coalescence,

Received: June 3, 2014
Published: July 17, 2014

   dx.doi.org/10.1021/ja505541q | J. Am. Chem. Soc. 2014, 136, 11121−11127

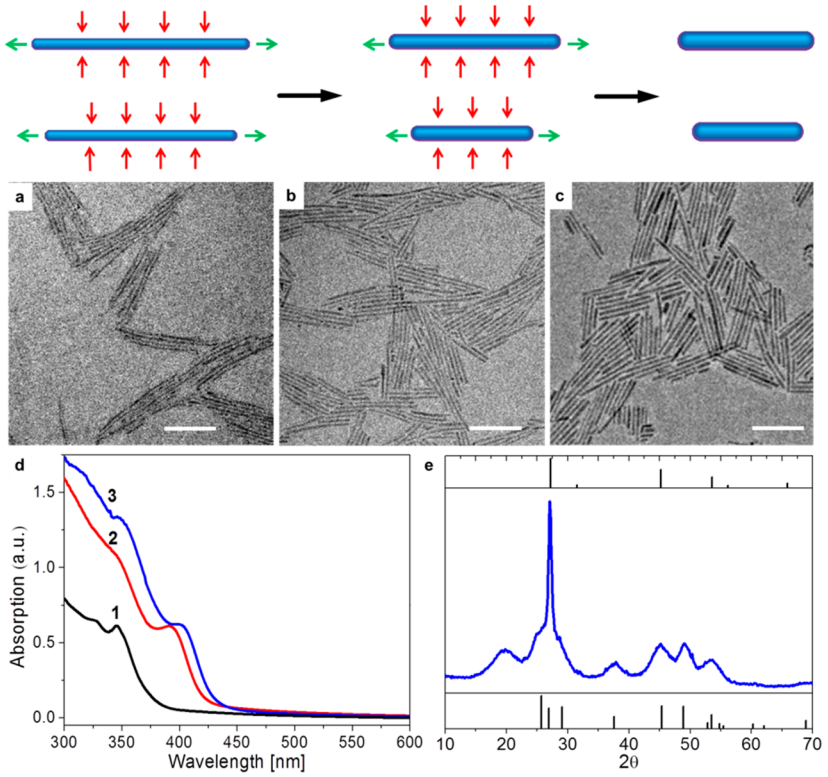


**Figure 1.** Evolution of ZnSe quantum rods from ZnSe nanowires. (top) Mechanism associated with the evolution from nanowires to nanorods via ripening. Green arrows represent the dissolution of monomers from the end facets into the solution, and red arrows represent the growth of monomers onto the side facets from the solution. (a–c) TEM images of the original ZnSe nanowires (a) and the ZnSe quantum rods evolved from the nanowires after 5 min (b) and 15 min (c) at 280 °C. All scale bars are 50 nm. (d) Absorption spectra of ZnSe nanocrystals. Curves 1–3 correspond to the materials shown in (a–c), respectively. (e) XRD pattern of the sample shown in (c). The broad band at ~20° in the XRD pattern is due to the diffraction of oleylamine ligand. The standard XRD patterns of cubic (top) and hexagonal (bottom) ZnSe are given for reference.

which are kinetically controlled,[8,51−53] in the present work we have developed a general strategy for the synthesis of quasi-1D ZnSe quantum rods with controlled aspect ratios from their respective nanowire counterparts by means of a ripening process via thermodynamically driven material diffusion. Interestingly in this context, we note the reports on atomic reconstruction processes in nanocrystals occurring at elevated temperature in vacuum.[54−57] Significant structural and morphological reconstructions were observed for single nanocrystals and core/shell heterostructures.

Besides ZnSe, we have also demonstrated that this strategy can be applied to produce quantum rods of other zinc chalcogenides, including ZnS and ZnTe, suggesting that this strategy is general and could be instructive for the synthesis of other quasi-1D nanostructures via colloidal synthesis.

## EXPERIMENTAL SECTION

**Chemicals.** $Zn(NO_3)_2{\cdot}6H_2O$ (99%), zinc diethyldithiocarbamate (97%), $ZnCl_2$ (99.995%), lithium triethylborohydride (1 M in tetrahydrofuran), trioctylphosphine (TOP) (90%), chloroform (99% anhydrous), toluene (99% anhydrous), and methanol (99.8% anhydrous) were purchased from Sigma-Aldrich. Selenium powder (99.999%) and tellurium powder (99.999%) were purchased from Strem Chemicals. Oleylamine (approximate $C_{18}$ content 80–90%) was purchased from Acros. All chemicals were used as received without further purification.

**Synthesis of ZnSe Nanowires.** ZnSe nanowires were synthesized according to a previously reported approach.[49] In a typical synthesis, 0.2 mmol (59.5 mg) of $Zn(NO_3)_2{\cdot}6H_2O$ and 30 mL of oleylamine were mixed in a three-neck flask. The mixture was degassed and refilled with Ar three times at room temperature and then heated to 110 °C and kept at this temperature for 0.5 h. At 160 °C, 2 mL of a 0.1 M solution of Se in oleylamine was injected into the flask. After the injection, the temperature was set at 120 °C, and the mixture was degassed for 10 min. Then the temperature was raised to 230 °C in 6 min. After 20 min at 230 °C, the reaction was quenched by removing the heating mantle.

**Synthesis of ZnS Nanowires.** ZnS nanowire were synthesized according to a previously reported approach with some modifications.[47] In a typical synthesis, 0.05 mmol (18 mg) of zinc diethyldithiocarbamate and 10 mL of oleylamine were mixed in a three-neck flask. The mixture was degassed and refilled with Ar three times at room temperature and then heated to 110 °C and kept at this temperature for 0.5 h. Then the temperature was raised from 110 to 230 °C in 6 min. After 20 min at 230 °C, the reaction was quenched by removing the heating mantle.

**Synthesis of ZnTe Nanowires.** ZnTe nanowires were synthesized according to a previously reported approach with some modifications.[58] In a typical synthesis, 0.2 mmol (27.3 mg) of $ZnCl_2$ and 10 mL of oleylamine were mixed in a three-neck flask. The mixture was degassed and refilled with Ar three times at room temperature and then heated to 110 °C and kept at this temperature for 0.5 h. A 0.5 M tellurium stock solution was prepared by dissolving tellurium powder into TOP at 280 °C. A 0.4 mL aliquot of this solution was mixed with 0.34 mL of lithium triethylborohydride (1 M in tetrahydrofuran) and 1 mL of oleylamine in the glovebox, and then the mixture was injected into the flask at 160 °C. After the injection, the temperature was set at 120 °C, and the mixture was degassed for 10 min. Then the temperature was raised from 120 to 230 °C in 6 min. After 20 min at 230 °C, the reaction was quenched by removing the heating mantle.

**Purification of Zinc Chalcogenide Nanowires.** The crude zinc chalcogenide nanowire product solution was dissolved in chloroform, and the nanowires were precipitated by adding methanol with the aid of centrifugation.


dx.doi.org/10.1021/ja505541q | J. Am. Chem. Soc. 2014, 136, 11121−11127

**Aging of ZnSe Nanowires.** After the purification, ZnSe nanowires were redissolved in oleylamine, and then the reaction solution was kept in the glovebox at room temperature for 2−4 weeks prior to the synthesis of ZnSe quantum rods.

**Synthesis of Zinc Chalcogenide Quantum Rods.** Purified zinc chalcogenide nanowires were redissolved in oleylamine in a three-neck flask. The reaction mixture was degassed and refilled with Ar three times at room temperature and then heated to 110 °C and kept at this temperature for 10 min. Then the reaction solution was heated to 280 °C in 10 min and kept at this temperature for 5−60 min. Aliquots were taken from time to time. The reaction was terminated by removing the heating mantle.

**Preparation of Zinc Precursor Stock Solution.** A 0.067 M zinc stock solution was prepared by dissolving 0.2 mmol (27.3 mg) of $ZnCl_2$ and 10 mL of oleylamine in a three-neck flask. The mixture was degassed and refilled with Ar three times at room temperature and then heated to 110 °C and kept at this temperature for 0.5 h.

**Sample Characterization.** UV−vis−NIR absorption spectroscopy was performed on a JASCO V-570 spectrometer using quartz cuvettes. Powder X-ray diffraction (XRD) patterns were obtained using Cu K$\alpha$ photons from a Phillips PW1830/40 diffractometer operated at 40 kV and 30 mA. Each sample was deposited as a thin layer on a low-background-scattering quartz substrate. Transmission electron microscopy (TEM) grids were prepared by depositing one drop of a solution of purified nanoparticles onto a standard carbon-coated grid. TEM was performed using a Tecnai $G^2$ Spirit Twin T-12 transmission electron microscope with a tungsten filament running at an accelerating voltage of 120 keV. High-resolution TEM (HRTEM) was performed using a Tecnai F20 $G^2$ high-resolution transmission electron microscope running at an accelerating voltage of 200 keV with a field-emission gun as an electron source.

## RESULTS AND DISCUSSION

Our strategy for synthesizing zinc chalcogenide quantum rods is based on a colloidal chemical synthetic approach. The synthetic protocol is illustrated in the flowchart in Figure 1. This strategy starts with the synthesis of ultrathin nanowires. Then the wires are purified from the growth solution and brought back into a reaction medium. In the second step, at an elevated temperature, the monomers dissolve into the solution preferentially from the end facets of the nanowires, which are the least stable regions, and meanwhile they grow onto the side facets of the nanowires, forming quantum rods via a ripening process[8,51] (Figure 1 top). We note that the classification of "wire" versus "rod" is defined herein by the reaction stage, whereby the first stage leads to thin nanowires and the second step to thick quantum rods.

We used ZnSe as an illustrative example of this strategy to substantiate the proposed mechanism. Details of the synthesis of ZnSe nanowires were provided in the Experimental Section, and this synthetic approach produced nearly monodispersed ZnSe nanowires (see the TEM image in Figure 1a) with a uniform diameter of 2.4 ± 0.3 nm (see the histograms in Figure 2a).

In the next step, we conducted the synthesis of ZnSe quantum rods starting with long ZnSe nanowires (length = 90 ± 16 nm; Figure 1a). The produced ZnSe nanowires were separated from the growth solution by dilution with chloroform and precipitation by methanol and then redissolved in oleylamine. The reaction mixture was heated to 280 °C. Within 5−15 min at 280 °C, TEM measurements on aliquots showed shrinkage along the long axis of the original ZnSe nanowires and expansion along the short axis, producing nearly monodispersed ZnSe quantum rods (Figure 1b,c). Starting with long ZnSe nanowires (length = 90 ± 16 nm, width = 2.4 ± 0.3 nm; Figures 1a and 2a), the length of the products shrunk to 52 ± 19 nm while the width increased to 3.5 ± 0.5 nm as the reaction evolved for 5 min at 280 °C (Figures 1b and 2b). Further reaction at this temperature for 20 min produced ZnSe quantum rods with a width of 4.2 ± 0.6 nm and a length of 40 ± 19 nm (Figures 1c and 2c). Accordingly, the absorption onset was red-shifted from 345 to 393 nm and then to 404 nm after 5 and 15 min at 280 °C, respectively (Figure 1d), in agreement with the increase in the width of the produced ZnSe quantum rods. The XRD pattern (Figure 1e) matches that of the hexagonal wurtzite ZnSe structure. The sharp feature at 27° in the XRD pattern associated with the (002) plane indicates that the long axis of the ZnSe nanorods corresponds to the crystallographic *c* axis of the wurtzite structure.

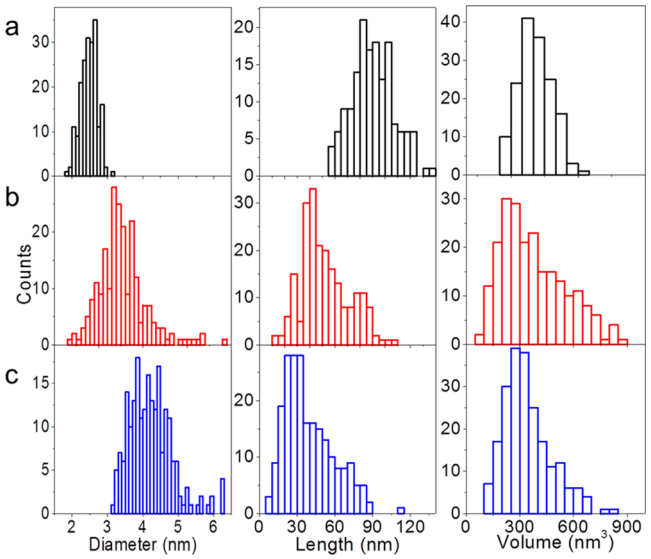


**Figure 2.** Size histograms of diameter (left frames), length (middle frames), and volume (right frames) of the original ZnSe nanowires (a) and ZnSe quantum rods after 5 min (b) and 15 min (c) at 280 °C, shown in Figure 1a−c, respectively.

In addition to the size histograms for the width and length of the produced ZnSe quantum rods, those for the volume enable us to perform a quantitative analysis in order to further support the mechanism of formation of ZnSe quantum rods from their nanowire counterparts (Figure 2). The TEM characterizations (Figure 1) show that the width and length of the produced ZnSe quantum rods dramatically changed. However, their volumes varied only slightly over a small range (from 410 to 360 nm$^3$) for the synthesis starting with long nanowires (Figure 2).

It is important to note that for thermodynamically driven material diffusion, the temperature of the reaction system should be high enough to overcome the activation barrier between the ZnSe nanowires and ZnSe quantum rods. We conducted several similar syntheses of ZnSe quantum rods from ZnSe nanowires at a variety of temperatures (160, 260, and 310 °C). The synthesis conducted at 160 °C did not lead to a change in the dimensions of the original ZnSe nanowires, which indicates that the reaction temperature of the system was insufficient to provide the activation energy, whereas syntheses performed at 260 and 310 °C produced short and thick ZnSe quantum rods. These results demonstrate that the material diffusion process, in which the evolution from long and thin ZnSe nanowires to short and thick quantum rods occurs, is thermodynamically controlled.


dx.doi.org/10.1021/ja505541q | J. Am. Chem. Soc. 2014, 136, 11121−11127

Compared with the growth mechanism of cadmium chalcogenide quantum rods, which is a highly kinetically controlled reaction,[51] the evolution of ZnSe quantum rods from their nanowire counterparts is a thermodynamically driven process. The rod formation mechanism in this case is illustrated in the scheme at the top of Figure 1. Starting from the thin nanowires, at an elevated temperature the monomers dissolve into the solution preferentially from the end facets of the nanowires. This preferential reactivity is related to the fact that the end facets are the least stable regions. At the same time, growth onto the side facets of the nanowires occurs, leading effectively to material redistribution. Therefore, shorter and thicker quantum rods are formed from the long and thin nanowires via a ripening process. This is the first time that this mechanism has been employed to synthesize colloidal quasi-1D semiconductor nanocrystals.

We also conducted the synthesis of ZnSe quantum rods starting with short ZnSe nanowires (length = 45 ± 14 nm, width = 2.4 ± 0.3 nm; Figure 3a). In this synthesis, as the reaction proceeded for 20 min at 280 °C, the length of the products shrank to 15 ± 5 nm while the diameter increased to 3.3 ± 0.4 nm (Figure 3b). Further reaction at this temperature for 60 min produced relatively short quantum rods with a length of 13 ± 5 nm and a width of 3.9 ± 0.7 nm (Figure 3c). The changes in the width of the nanoparticles are manifested in a red shift in the absorption onset from 345 to 385 nm and then to 401 nm after 20 and 60 min at 280 °C, respectively (Figure 3d). The volumes of ZnSe nanocrystals in this case also were only slightly reduced from 161 $nm^3$ for the short nanowires to 136 $nm^3$ for the final products (Figure 3), consistent with the growth mechanism proposed above. The XRD pattern (Figure 3e) matches that of hexagonal wurtzite ZnSe, and the sharp feature of the (002) plane corroborates the direction of the long axis. The combination of the synthesis of ZnSe quantum rods starting with long ZnSe nanowires as described above and the synthesis starting with short nanowires described here demonstrates that control of the width and aspect ratio (Figure S1 in the Supporting Information) of quasi-1D ZnSe nanocrystals can be successfully achieved by this strategy.

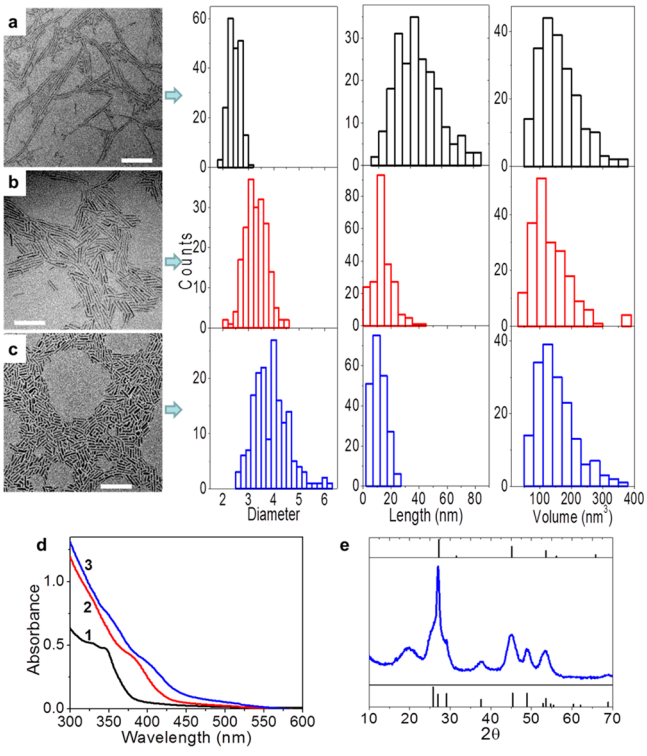


**Figure 3.** Evolution of ZnSe quantum rods from short ZnSe nanowires. (a–c) TEM images and size histograms for diameter, length, and volume of the original ZnSe nanowires (a) and the ZnSe quantum rods evolved from the nanowires after 20 min (b) and 60 min (c) at 280 °C. All scale bars are 50 nm. (d) Absorption spectra of ZnSe nanocrystals. Curves 1–3 correspond to the materials shown in (a–c), respectively. (e) XRD pattern of the sample shown in (c). The broad band at ~20° in the XRD pattern is due to the diffraction of oleylamine ligand. The standard XRD patterns of cubic (top) and hexagonal (bottom) ZnSe are given for reference.

An interesting question relates to what might be the end product of this ripening process at long times. To address this, we performed the synthesis of ZnSe quantum rods starting with long ZnSe nanowires, similar to those in Figure 1a, using reaction times of up to 60 min at 280 °C, as shown in Figure S2. After 15 min at 280 °C, ZnSe quantum rods were obtained, and the corresponding absorption spectrum manifests an onset at 400 nm (Figure S2a,d). Further reaction of the quantum rods at this temperature for another 15 min led to the formation of short rods and dots (Figure S2b). The corresponding absorption spectrum is similar to that of the preceding product in Figure S2a, along with slight scattering in the visible range. When the reaction evolved for 60 min at 280 °C, the products decomposed, as evidenced by the TEM images in Figure S2c and also the featureless absorption spectrum in Figure S2d.

It is important to note that a modified approach of the synthetic route discussed here leads to the formation of ZnSe rod couples, as recently reported by us.[49] The synthesis of rod couples, reported elsewhere, starts with a similar synthesis of thin ZnSe nanowires at lower temperature. However, the rod couples are obtained when the reaction mixture is directly heated to the high temperature without the purification of excess monomers. In this case, the presence of excess monomers in the solution partially suppresses the ripening of wires into rods. At the same time, it allows for the formation of connecting regions between two nanorods at their edges. In contrast, for the nanorod synthesis described herein, monomer removal is essential and enables the nanowires to form nanorods via ripening. This important point is further discussed below.

Starting the synthesis of ZnSe quantum rods with aged ZnSe nanowires that had been kept in oleylamine at room temperature for 2–4 weeks significantly improved the size distribution of the produced ZnSe quantum rods (Figure 4). Compared with the as-prepared ZnSe nanowires, no obvious changes in the dimensions of the aged nanowires were observed, but the absorption onset of the aged ZnSe nanowires showed a slight red shift and lost the sharp excitonic absorption feature (Figure S3).

In addition to Figure 4a, Figure 5 shows TEM images of ZnSe quantum rods synthesized starting with aged nanowires, and the corresponding size histograms are shown in Figure S4. The lengths of the produced ZnSe quantum rods ranged from 26 to 95 nm, and the widths ranged from 3.5 to 4.2 nm. Starting with the aged ZnSe nanowires, our strategy produced ZnSe quantum rods with good size distributions, presenting controlled widths and lengths.


dx.doi.org/10.1021/ja505541q | J. Am. Chem. Soc. 2014, 136, 11121–11127

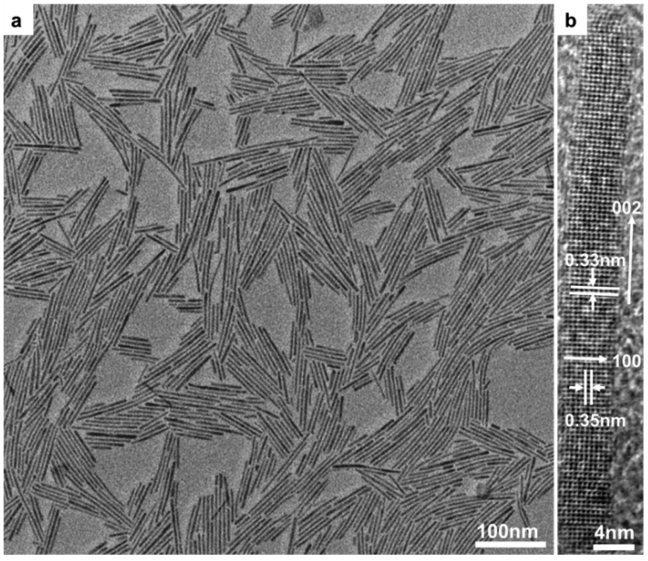


**Figure 4.** (a) TEM and (b) HRTEM images of ZnSe quantum rods (width × length: 3.8 ± 0.4 nm × 55 ± 19 nm) synthesized from ZnSe nanowires aged at room temperature for 4 weeks (width × length: 2.4 ± 0.3 nm × 137 ± 25 nm). The images reveal that aging of the ZnSe nanowires improves the size distribution of ZnSe quantum rods. The arrow in (b) indicates that the orientation of the long axis of the ZnSe quantum rods is parallel to the crystallographic *c* axis of the hexagonal wurtzite structure.

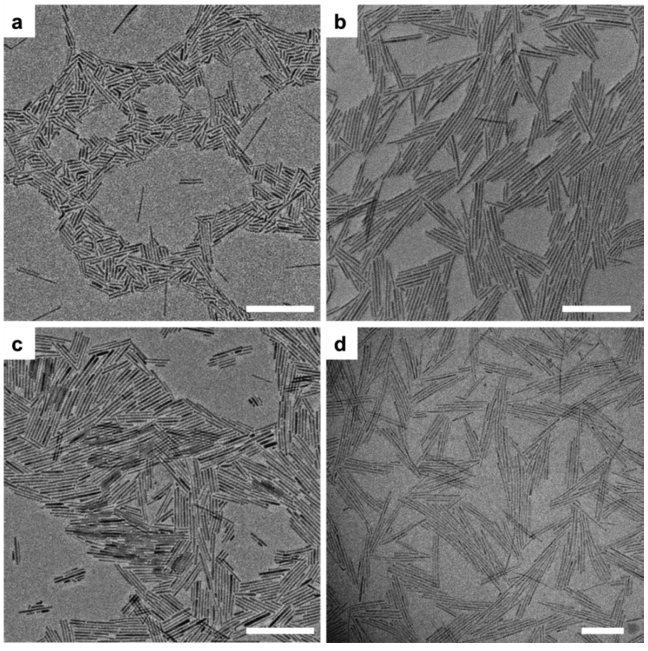


**Figure 5.** TEM images of ZnSe quantum rods synthesized starting with aged ZnSe nanowires. All scale bars are 50 nm. Diameter × length: (a) 3.5 ± 0.3 nm × 26 ± 7 nm; (b) 3.8 ± 0.4 nm × 62 ± 25 nm; (c) 4.2 ± 0.6 nm × 52 ± 19 nm; (d) 3.5 ± 0.3 nm × 95 ± 17 nm.

The HRTEM measurement (Figure 4b) shows that the quantum rods are single-crystalline, and the lattice plane spacings extracted from the fast Fourier transform (FFT) analysis of selected areas are 0.33 nm for (*hkl*) = (002) and 0.35 nm for (*hkl*) = (100). These two planes are perpendicular to each other, typical of a hexagonal wurtzite ZnSe structure. The perpendicular orientation of the (002) plane with respect to the long axis of the quantum rods is consistent with the sharp features of the (002) plane in the XRD patterns, which corresponds well to the hexagonal ZnSe structure (Figures 1e and 3e).

To further demonstrate the generality of this strategy, it was employed to synthesize quantum rods of other zinc chalcogenides, including ZnS and ZnTe, starting from their respective nanowire counterparts. ZnS (Figure 6a) and ZnTe

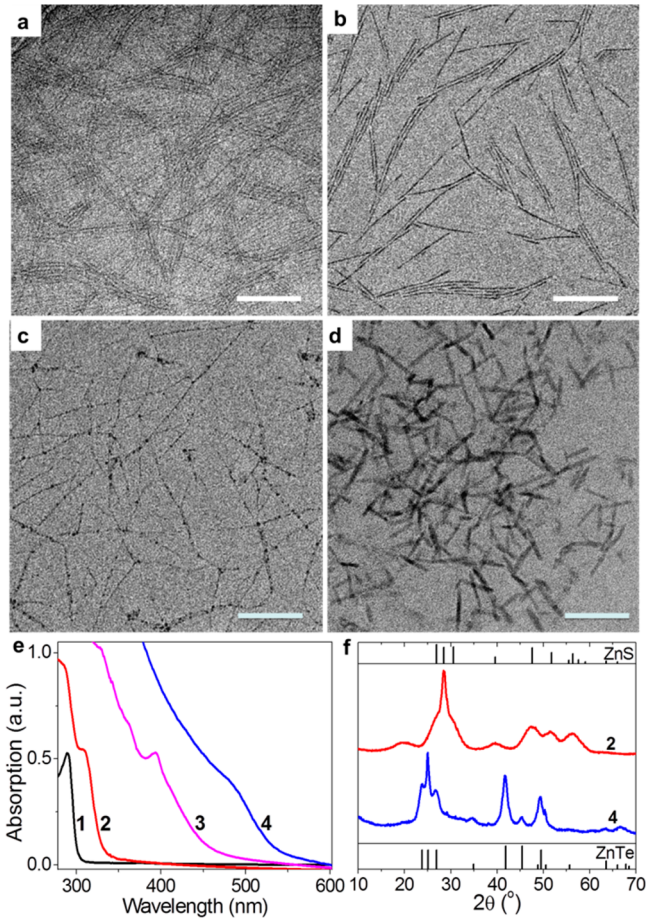


**Figure 6.** ZnS and ZnTe quantum rods evolved from ZnS and ZnTe nanowires. (a–d) TEM images of ZnS nanowires (a), ZnS quantum rods evolved from the nanowires in (a) after 30 min at 280 °C (b), ZnTe nanowires (c), and ZnTe quantum rods evolved from the nanowires in (c) after 30 min at 280 °C (d). All scale bars are 50 nm. (e) Absorption spectra of ZnS and ZnTe nanocrystals. Curves 1–4 correspond to the materials shown in (a–d), respectively. (f) XRD patterns of ZnS and ZnTe quantum rods. Curves 2 and 4 correspond to the samples shown in (b) and (d), respectively. The broad band at ~20° in the XRD pattern is due to the diffraction of oleylamine ligand. The standard XRD patterns for hexagonal wurtzite ZnS and ZnTe are given for reference.

nanowires (Figure 6c) with diameters of ~2 nm were prepared via colloidal chemical synthetic approaches (see the Experimental Section for details), and their absorption spectra manifested band gaps at 290 and 394 nm, respectively (Figure 6e). As the reaction evolved for 30 min at 280 °C, ZnS quantum rods (with a diameter of ~3.5 nm; Figure 6b) and ZnTe quantum rods (with a diameter of ~4.5 nm; Figure 6d) were produced. The changes in the widths of the quantum rods are manifested by the red shifts in the absorption onsets to 310 and 490 nm for ZnS and ZnTe, respectively (Figure 6e). XRD


dx.doi.org/10.1021/ja505541q | J. Am. Chem. Soc. 2014, 136, 11121–11127

characterization showed that the produced ZnS and ZnTe quantum rods have hexagonal wurtzite structures with preferential elongation along the (002) lattice plane (Figure 6f).

Combination of the results for the synthesis of ZnS and ZnTe quantum rods with those for ZnSe clearly demonstrates that the thermodynamically driven ripening-based synthetic strategy is general and can successfully circumvent the limitation of the width control of quasi-1D nanocrystals imposed by alkylamines, generating zinc chalcogenide quantum rods with controlled aspect ratios.

The proposed ripening mechanism was further investigated by experiments with deliberate addition of excess Zn precursors prior to the high-temperature phase. This may affect the ripening process, since the formation of zinc chalcogenide quantum rods is associated with the dissolution of monomers from the end facets of the nanoparticles into the solution, diffusion in solution, and growth of monomers onto the side facets of the nanoparticles from the solution. To this end, we performed the synthesis starting with a mixture containing both ZnSe nanowires and excess zinc precursor (see the Experimental Section for details). This synthesis is analogous to the purification and readdition of monomer approach used previously by us, which enabled us to achieve good control over the characteristics of ZnSe nanorod couples.[49] We anticipated that the ripening of ZnSe nanowires would be inhibited in the presence of zinc monomer if the formation of quantum rods is based on a ripening process via the reaction solution.

The synthetic conditions were exactly the same as those addressed in the Experimental Section for the synthesis of ZnSe quantum rods except that the starting material was a mixture containing both ZnSe nanowires and zinc oleylamine stock solution. As the reaction evolved for 10 min at 280 °C, the diameter of the produced nanoparticles became slightly larger than that of the original ZnSe nanowires (Figure S5b), and the absorption onset was slightly red-shifted from 345 to 356 nm (Figure S5d). Further reaction at this temperature for 45 min did not change the dimensions of the nanocrystals much (Figure S5c), and the absorption onset had only a rather small further red shift from 356 to 366 nm (Figure S5d). This demonstrates that the ripening process of the ZnSe nanowires was significantly hindered in the presence of zinc precursors. This suggests that the ripening mechanism leading to the formation of zinc chalcogenide quantum rods from their nanowires counterparts is a thermodynamically driven material diffusion process via solution.

## CONCLUSIONS

In conclusion, we have developed a strategy for the synthesis of zinc chalcogenide quantum rods with controlled aspect ratios. The mechanism of the formation of zinc chalcogenide quantum rods involves a ripening process by thermodynamically driven material diffusion in solution. Furthermore, this synthetic technique is based on a phosphine-free colloidal method. The availability of "green" zinc chalcogenide quantum rods synthesized through this strategy paves the way for their future applications in optics, photocatalysis, electronic devices, and biolabeling.

## ASSOCIATED CONTENT

### Supporting Information

Aspect ratio evolution of quasi-1D nanocrystals; evolution of ZnSe nanocrystals as a function of reaction time at elevated temperature; TEM images, absorption spectra, and size histograms for ZnSe quantum rod synthesis starting with the aged ZnSe nanowires; and TEM images and absorption spectra associated with the evolution of ZnSe nanowires in the presence of zinc precursors. This material is available free of charge via the Internet at http://pubs.acs.org.

## AUTHOR INFORMATION

### Corresponding Author

uri.banin@mail.huji.ac.il

### Notes

The authors declare no competing financial interest.

## ACKNOWLEDGMENTS

The research leading to these results received funding from the European Research Council under the European Union's Seventh Framework Programme (FP7/2007-2013)/ERC Grant Agreement 246841. U.B. thanks the Alfred and Erica Larisch Memorial Chair. G.J. thanks the National Natural Science Foundation of China (Grant 11004177) for travel support. We acknowledge the use of the facilities of the Unit for Nanocharacterization in the Center for Nanoscience and Nanotechnology at Hebrew University and thank Dr. Inna Popov for her assistance in the TEM characterization. We also thank Dr. Shany Neyshtadt for insightful discussions.

## REFERENCES

(1) Xia, Y.; Yang, P.; Sun, Y.; Wu, Y.; Mayers, B.; Gates, B.; Yin, Y.; Kim, F.; Yan, H. *Adv. Mater.* **2003**, *15*, 353.
(2) Yin, Y.; Alivisatos, A. P. *Nature* **2005**, *437*, 664.
(3) Kwon, S. G.; Hyeon, T. *Acc. Chem. Res.* **2008**, *41*, 1696.
(4) Puzder, A.; Williamson, A. J.; Zaitseva, N.; Galli, G.; Manna, L.; Alivisatos, A. P. *Nano Lett.* **2004**, *4*, 2361.
(5) Penn, R. L.; Banfield, J. F. *Science* **1998**, *281*, 969.
(6) Banfield, J. F.; Welch, S. A.; Zhang, H.; Ebert, T. T.; Penn, R. L. *Science* **2000**, *289*, 751.
(7) Peng, X.; Manna, L.; Yang, W.; Wickham, J.; Scher, E.; Kadavanich, A.; Alivisatos, A. P. *Nature* **2000**, *404*, 59.
(8) Peng, Z. A.; Peng, X. *J. Am. Chem. Soc.* **2001**, *123*, 1389.
(9) Manna, L.; Scher, E. C.; Alivisatos, A. P. *J. Am. Chem. Soc.* **2000**, *122*, 12700.
(10) Pacholski, C.; Kornowski, A.; Weller, H. *Angew. Chem., Int. Ed.* **2002**, *41*, 1188.
(11) Cho, K. S.; Talapin, D. V.; Gaschler, W.; Murray, C. B. *J. Am. Chem. Soc.* **2005**, *127*, 7140.
(12) Yu, J. H.; Joo, J.; Park, H. M.; Baik, S. I.; Kim, Y. W.; Kim, S. C.; Hyeon, T. *J. Am. Chem. Soc.* **2005**, *127*, 5662.
(13) Koh, W. K.; Bartnik, A. C.; Wise, F. W.; Murray, C. B. *J. Am. Chem. Soc.* **2010**, *132*, 3909.
(14) Liao, H. G.; Cui, L.; Whitelam, S.; Zheng, H. *Science* **2012**, *336*, 1011.
(15) Li, D.; Nielson, M. H.; Lee, J. R. I.; Frandsen, C.; Banfield, J. F.; De Yoreo, J. J. *Science* **2012**, *336*, 1014.
(16) Evers, W. H.; Goris, B.; Bals, S.; Casavola, M.; De Graaf, J.; van Roij, R.; Dijkstra, M.; Vanmaekelbergh, D. *Nano Lett.* **2013**, *13*, 2317.
(17) Hu, J.; Li, L. S.; Yang, W.; Manna, L.; Wang, L. W.; Alivisatos, A. P. *Science* **2001**, *292*, 2060.
(18) Mokari, T.; Rothenberg, E.; Popov, I.; Costi, R.; Banin, U. *Science* **2004**, *304*, 1787.
(19) Mokari, T.; Sztrum, C. G.; Salant, A.; Rabani, E.; Banin, U. *Nat. Mater.* **2005**, *4*, 855.
(20) Milliron, D. J.; Hughes, S. M.; Cui, Y.; Manna, L.; Li, J.; Wang, L. W.; Alivisatos, A. P. *Nature* **2004**, *430*, 190.
(21) Gur, I.; Fromer, N. A.; Geier, M. L.; Alivisatos, A. P. *Science* **2005**, *310*, 462.

(22) Carbone, L.; Nobile, C.; De Giorgi, M.; Sala, F. D.; Morello, G.; Pompa, P.; Hytch, M.; Snoeck, E.; Fiore, A.; Franchini, I. R.; Nadasan, M.; Silvestre, A. F.; Chiodo, L.; Kudera, S.; Cingolani, R.; Krahne, R.; Manna, L. *Nano Lett.* **2007**, *7*, 2942.
(23) Talapin, D. V.; Nelson, J. H.; Shevchenko, E. V.; Aloni, S.; Sadtler, B.; Alivisatos, A. P. *Nano Lett.* **2007**, *7*, 2951.
(24) Sitt, A.; Salant, A.; Menagen, G.; Banin, U. *Nano Lett.* **2011**, *11*, 2054.
(25) Borys, N. J.; Walter, M. J.; Huang, J.; Talapin, D. V.; Lupton, J. M. *Science* **2010**, *330*, 1371.
(26) Wang, T.; Zhuang, J.; Lynch, J.; Chen, O.; Wang, Z.; Wang, X.; LaMontagne, D.; Wu, H.; Wang, Z.; Cao, Y. C. *Science* **2012**, *338*, 358.
(27) Tang, Z.; Kotov, N. A.; Giersig, M. *Science* **2002**, *297*, 237.
(28) Tang, Z.; Zhang, Z.; Wang, Y.; Glotzer, S. C.; Kotov, N. A. *Science* **2006**, *314*, 274.
(29) Srivastava, S.; Santos, A.; Critchley, K.; Kim, K. S.; Podsiadlo, P.; Sun, K.; Lee, J.; Xu, C.; Lilly, G. D.; Glotzer, S. C.; Kotov, N. A. *Science* **2010**, *327*, 1355.
(30) Sun, J.; Wang, L. W.; Buhro, W. E. *J. Am. Chem. Soc.* **2008**, *130*, 7997.
(31) Talapin, D. V.; Rogach, A. L.; Shevchenko, E. V.; Kornowski, A.; Haase, M.; Weller, H. *J. Am. Chem. Soc.* **2002**, *124*, 5782.
(32) Li, H.; Zanella, M.; Genovese, A.; Povia, M.; Falqui, A.; Giannini, C.; Manna, L. *Nano Lett.* **2011**, *11*, 4964.
(33) Li, H.; Brescia, R.; Krahne, R.; Bertoni, G.; Alcocer, M. J. P.; D'Andrea, C.; Scotognella, F.; Tassone, F.; Zanella, M.; De Giorgi, M.; Manna, L. *ACS Nano* **2012**, *6*, 1637.
(34) Li, L. S.; Pradhan, N.; Wang, Y.; Peng, X. *Nano Lett.* **2004**, *4*, 2261.
(35) Li, Y.; Li, X.; Yang, C.; Li, Y. *J. Phys. Chem. B* **2004**, *108*, 16002.
(36) Cozzoli, P. D.; Manna, L.; Curri, M. L.; Kudera, S.; Giannini, C.; Striccoli, M.; Agostiano, A. *Chem. Mater.* **2005**, *17*, 1296.
(37) Yao, T.; Zhao, Q.; Qiao, Z.; Peng, F.; Wang, H.; Yu, H.; Chi, C.; Yang, J. *Chem.—Eur. J.* **2011**, *17*, 8663.
(38) Pradhan, N.; Efrima, S. *J. Phys. Chem. B* **2004**, *108*, 11964.
(39) Acharya, S.; Efrima, S. *J. Am. Chem. Soc.* **2005**, *127*, 3486.
(40) Panda, A. B.; Acharya, S.; Efrima, S. *Adv. Mater.* **2005**, *17*, 2471.
(41) Zhang, J.; Chen, P. C.; Shen, G.; He, J.; Kumbhar, A.; Zhou, C.; Fang, J. *Angew. Chem. Int. Ed.* **2008**, *47*, 9469.
(42) Deng, Z.; Tong, L.; Flores, M.; Lin, S.; Cheng, J. X.; Yan, H.; Liu, Y. *J. Am. Chem. Soc.* **2011**, *133*, 5389.
(43) Zhang, J.; Sun, K.; Kumbhar, A.; Fang, J. *J. Phys. Chem. C* **2008**, *112*, 5454.
(44) Chin, P. T. K.; Stouwdam, J. W.; Janssen, R. A. J. *Nano Lett.* **2009**, *9*, 745.
(45) Deng, Z.; Yan, H.; Liu, Y. *Angew. Chem. Int. Ed.* **2010**, *49*, 8695.
(46) Zhu, G.; Zhang, S.; Xu, Z.; Ma, J.; Shen, X. *J. Am. Chem. Soc.* **2011**, *133*, 15605.
(47) Zhang, Y.; Xu, H.; Wang, Q. *Chem. Commun.* **2010**, *46*, 8941.
(48) Hou, L.; Zhang, Q.; Ling, L.; Li, C. X.; Chen, L.; Chen, S. *J. Am. Chem. Soc.* **2013**, *135*, 10618.
(49) Jia, G.; Sitt, A.; Hitin, G. B.; Hadar, I.; Bekenstein, Y.; Amit, Y.; Popov, I.; Banin, U. *Nat. Mater.* **2014**, *13*, 301.
(50) Acharya, S.; Sarkar, S.; Pradhan, N. *J. Phys. Chem. C* **2013**, *117*, 6006.
(51) Peng, Z. A.; Peng, X. *J. Am. Chem. Soc.* **2002**, *124*, 3343.
(52) Lee, S. M.; Cho, S. N.; Cheon, J. *Adv. Mater.* **2003**, *15*, 441.
(53) Jun, Y. W.; Choi, J. S.; Cheon, J. *Angew. Chem. Int. Ed.* **2006**, *45*, 3414.
(54) van Huis, M. A.; Young, N. P.; Pandraud, G.; Greemer, J. F.; Vanmaekelbergh, D.; Kirkland, A. I.; Zandbergen, H. W. *Adv. Mater.* **2009**, *21*, 4992.
(55) Grodzińska, D.; Pietra, F.; van Huis, M. A.; Vanmaekelbergh, D.; de Mello Donegá, C. *J. Mater. Chem.* **2011**, *21*, 11556.
(56) Yalcin, A. O.; de Nijs, B.; Fan, Z.; Tichelaar, F. D.; Vanmaekelbergh, D.; van Blaaderen, A.; Vlugt, T. J. H.; van Huis, M. A.; Zandbergen, H. W. *Nanotechnology* **2014**, *25*, 055601.
(57) Figuerola, A.; van Huis, M.; Zanella, M.; Genovese, A.; Marras, S.; Falqui, A.; Zandbergen, H. W.; Cingolani, R.; Manna, L. *Nano Lett.* **2010**, *10*, 3028.
(58) Zhang, J.; Jin, S.; Fry, H. C.; Peng, S.; Shevchenko, E.; Wiederrecht, G. P.; Rajh, T. *J. Am. Chem. Soc.* **2011**, *133*, 15324.